AN EFFICIENT TECHNIQUE FOR RAPID ESTIMATION OF FLOOD WATER LEVELS: COMBINING CYGNSS GNSS-R L1 DATA WITH DTMS

Z. Ma [1,2], S. Zhang [1], H. Park [2,3], A. Camps [2,3,4]

[1]College of Geological Engineering and Geomatics, Chang'an University, Xi'an 710054, China
[2]CommSensLab – UPC, Universitat Politècnica de Catalunya – BarcelonaTech, Barcelona, Spain
[3] Institut d'Estudis Espacials de Catalunya (IEEC) – CTE-UPC, E-08034 Barcelona, Spain
[4]ASPIRE Visiting International Professor, UAE University, CoE, POBox 15551 Al-Ain, UAE

ABSTRACT

Numerous studies have demonstrated the effectiveness of CYGNSS data for flood detection and mapping. However, the vast majority of the studies only focuses on flood extent detection, ignoring the importance of flood water levels in post-disaster relief. Meanwhile, most of the existing studies on inland water levels altimetry using CYGNSS data are based on the CYGNSS raw IF data using either the time-delay method or the phase method for altimetry. Although high accuracy can be obtained, at present the CYGNSS raw IF data is not a standard data, so it cannot be applied to the study of emergency flooding events. Given the above research gaps, this study proposes an effective method to combine CYGNSS L1 standard data with DTM for rapid estimation of flood water levels. The effectiveness of the proposed methodology is validated using the case of the 2022 Pakistan mega-flood. Comparison with ICESat-2 altimetry data gives encouraging results.

Index Terms— GNSS-R, CYGNSS, flood, water level, water extent

1. INTRODUCTION

NASA Cyclone Global Navigation Satellite System (CYGNSS) is a constellation of eight GNSS-R LEO micro-satellites launched in late 2016, each carrying on-board a GNSS-R payload. Each payload has four GPS L1-band signal tracking channels that can simultaneously receive four reflected signals from the Earth's surface. Currently, CYGNSS has demonstrated that it can be used for environmental parameter retrieval such as sea surface wind [1], sea surface wave height [2], soil moisture [3], and vegetation biomass [4]. Among them, in the last two years monitoring surface inundation using CYGNSS data is a hot research topic. Because it uses L-band signals transmitted by GPS satellites, CYGNSS is less susceptible to clouds and rain than optical remote sensing satellites. At the same time, the short revisit period gives CYGNSS a better chance to monitor short-term flood events than SAR satellites. The absence of a specialized transmitter also means that CYGNSS has a much lower cost than other traditional microwave remote sensing satellites. The above advantages make CYGNSS uniquely suited for flood monitoring.

However, most of the existing studies on flood monitoring using CYGNSS data have focused on flood extent mapping with very few studies focusing on flood water level [5], [6]. Nevertheless, flood water level is an important variable that should not be ignored in emergency response to flood disasters. Although some works in the literature have also investigated the feasibility of using CYGNSS data to retrieve the water levels of inland water bodies, most of them are based on the CYGNSS raw IF data, and use either time delay or phase altimetry [7], [8]. Considering that the raw IF data are not the standard data of CYGNSS, and that both the time delay and phase altimetry require a certain amount of computation, at the present time it is almost impossible to apply them to the retrieval of water level in short-term flooding events.

Inspired by [9], this study proposes a rapid retrieval method of flood water levels by combining CYGNSS L1 standard data with Digital Terrain Mode (DTM). The effectiveness of the proposed methodology is validated using the 2022 Pakistan mega flood as a case study. As compared to the IceSat-2 altimetry data, the bias of the CYGNSS results is about -0.2 m, the root mean squared error (RMSE) is about 1.39 m, and the correlation between the two is $R^2 > 0.98$. The above results preliminarily validate the effectiveness of the proposed method for rapid flood mapping.

2. DATA SOURCES AND METHODOLOGY

2.1. Approach to flood water level estimation by combining DTM data

Digital Terrain Model represents the bare ground without any objects, such as plants or buildings, and it is commonly used for applications such as flood or drainage modelling, land use studies, etc. The DTM data used in this study is FABDEM (Forest and Buildings removed Copernicus DEM), which is a global elevation map produced based on Copernicus GLO 30 Digital Elevation Model (DEM) data with building and tree bias removed. The data cover the globe and are provided in a

1 arc second grid size [10]. Figure 1 illustrates the flood water level estimation approach based on DTM data proposed in this study.

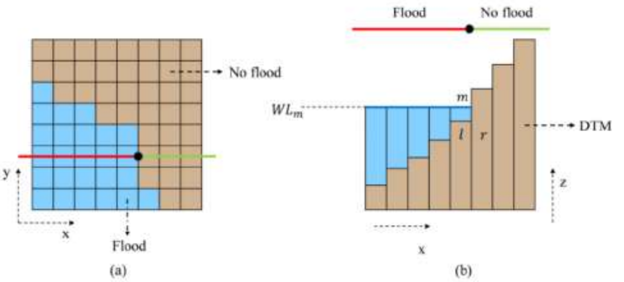

Fig. 1. Approach to estimate the flood water level by combining flood extension maps from CYGNSS L1 data and DTM data.

As it can be seen in Fig. 1, before using the flood water levels estimation method, the surface first needs to be categorized as flooded, and not flooded. After that, the DTM data is introduced to transform the 2D surface inundation map in plain view (Fig. 1(a)) into a 3D surface inundation map including water levels, as shown in Fig. 1(b). Following the determination of the boundaries of the flood extent (e.g., m in Fig. 1(b)), the water levels of m must fall between the DTM of l and r. Further approximation, i.e.:

$$WL_m \in [DTM_l, DTM_r] \approx mean(DTM_l, DTM_r) \qquad (1)$$

After obtaining the water levels at the boundaries, the water levels within the flood were derived by linearly interpolating the water levels at the boundaries. In this study the EGM2008 geoid undulations is used. The orthometric height of water surface is also referred to as water level. Given the unique advantages of CYGNSS data for flood monitoring, we choose to use CYGNSS data to differentiate between flooded and unflooded surfaces.

2.2. CYGNSS Surface Reflectivity

The CYGNSS data used in this study is the L1 Science Data Record Version 3.1 [11]. The basic CYGNSS observable is the Delay-Doppler Map (DDM). The DDM is generated from the reflections from the Earth's surface at different locations near the specular point (glistening zone), and its shape depends on the surface roughness and the relative motion of the CYGNSS satellites, the GPS satellites, and the Earth's topography. The signal-to-noise ratio (SNR) as well as the surface reflectivity (SR) obtained from the DDMs are highly sensitive to the presence of water bodies in the CYGNSS observation footprint. In general, the larger the proportion of calm water bodies in the observation footprint, the larger the proportion of coherent components in the reflected signal [12], [13], and the larger the SR and the SNR of CYGNSS. This is also the basic principle of flood detection (including inland water bodies) using CYGNSS L1 data.

This study utilizes the CYGNSS SR threshold method to differentiate the flooded state of a surface. That is, when the SR exceeds a certain threshold, the surface is considered to be flooded [5], [6], [14]. Besides the threshold method, some studies have proposed other methods, such as the change detection method [15], and the DDM coherence detection method [16], etc. Based on the results in [17], this study uses the SR of -11 dB as the threshold. Taking into account the spatial resolution of the CYGNSS L1 data, all observations are gridded to 3 km × 3 km in order to maintain a consistent spatial and temporal datum. This resolution is roughly the length of the dwell line per CYGNSS integration time (500 ms), and it is appropriate spatial resolution where there is a coherent reflection on ground [12],[18]. Meanwhile, due to the quasi-random spatial distribution properties of the CYGNSS L1 data, to obtain observations with high spatial and temporal resolution, the CYGNSS SR is interpolated every three days using spatial interpolation based on previous observations (POBI) [19]. Previous studies have demonstrated the effectiveness of POBI interpolation in the detection of short-term flood events from CYGNSS data [20].

2.3. ICESat-2 data

In order to validate the effectiveness of the method to combine CYGNSS L1 data with DTM information for rapid estimation of flood water levels, Ice, Cloud, and land Elevation Satellite 2 (ICESat-2) altimetry data were selected. ICESat-2 is part of NASA's Earth Observing Systems and is designed to measure ice-cap heights and sea-ice thickness, while also providing global topographic measurements of cities, lakes and reservoirs, oceans, and land surfaces. With its on-board lidar, Advanced Topographic Laser Altimeter System (ATLAS) and multiple pulses, ICESat-2 has a very high altimetry density (10,000 laser pulses a second). The ICESat-2 L3A Land and Vegetation Height V006 data is used in this study, and they can be downloaded through the National Snow & Ice Data Center (NSIDC) [21]. The surface along-track height data from this dataset is used.

3. RESULTS

The effectiveness of our methodology is validated by using the 2022 Pakistan mega-flood as a case study. Between June and October 2022, intense monsoon rains led to the worst floods in Pakistan's recorded history. The floods killed nearly 2,000 people, and caused economic losses of about $15 billion. The surface inundation distribution derived from CYGNSS SR for August 29-31 and September 2-4, 2022 is shown in Fig. 2.

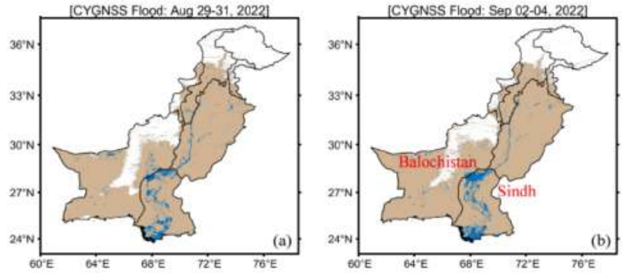

Fig. 2. Distribution of flood extent in Pakistan for August 29-31 and September 2-4, 2022 (derived from CYGNSS SR), with blue representing flooded and brown representing unflooded.

As it can be seen in Fig. 2, the floods occurred mainly in the Sindh province and the Balochistan province of Pakistan. The corresponding flood water levels are further calculated using the flood water levels estimation method incorporating DTM data presented in Section 2.1. The results of the flood water level retrieval are given in Fig. 3, along with the observation tracks of the ICESat-2 data used to validate CYGNSS results.

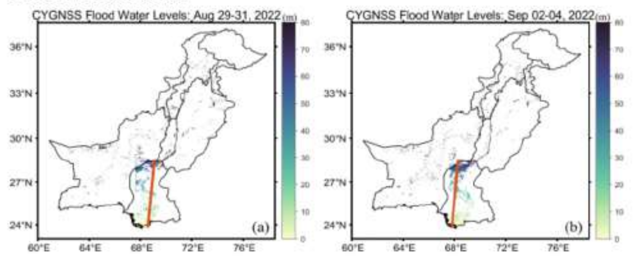

Fig. 3. Distribution of flood water levels in Pakistan on August 29-31 and September 2-4, 2022 (derived from CYGNSS SR maps combined with DTM data). Red lines represent the observation tracks of the corresponding ICESat-2 satellites used for validation. ICESat-2 data dates: (a) August 30, 2022; (b) September 3, 2022.

As it can be seen in Fig. 3, the proposed approach to combine CYGNSS SR, and DTM data successfully retrieved the water levels of Pakistan floods. Next, our results have been validated using ICESat-2 altimetry data. The comparison of ICESat-2 data with CYGNSS flood water levels retrieval is given in Fig. 4.

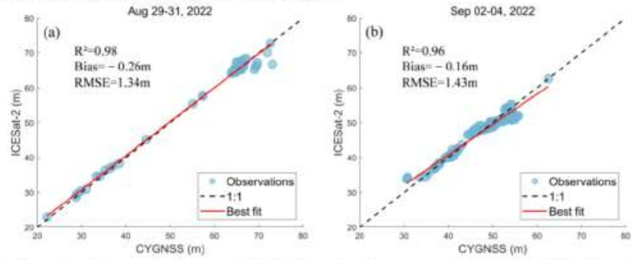

Fig. 4. Correlation of ICESat-2 data and CYGNSS flood water levels retrievals.

As seen in Fig. 4, the flood water level retrievals obtained by combining CYGNSS SR and DTM data are strongly correlated to ICESat-2 data ($R^2 > 0.98$). As compared to ICESat-2 data, the bias of the CYGNSS-derived results is about -0.2 m, and the RMSE is about 1.39 m. The good agreement between the CYGNSS results and the ICESat-2 data initially proves the effectiveness of our proposed method.

4. CONCLUSIONS

This study proposes an effective and fast flood water level retrieval technique by combining standard CYGNSS L1 data with DTM information. By introducing topographic information, flood monitoring results including water levels were successfully obtained. The high consistency of the comparison with ICESat-2 data in the 2022 Pakistan mega-flood case study provides the effectiveness of our approach.

In contrast to other existing methods using CYGNSS data to retrieve inland water levels, which mostly rely on raw IF data and require a significant amount of computation, our method is not only more efficient, but also uses CYGNSS L1 standard data, which allows for emergency monitoring of unexpected flood events [8], [22]. Moreover, as compared to the longer revisit period of other altimetry satellites (e.g., about 90 days for ICESat-2), the shorter revisit period of CYGNSS data (median/average revisit time of about 2.8h/7.2h) in conjunction with the POBI method [19], [20] will be an important complement to the existing satellite flood mapping capability and altimetry.

5. ACKNOWLEDGEMENTS

This research was funded by the National Natural Science Foundation of China Projects (Grant No.42074041); The National Key Research and Development Program of China (Grant No.2020YFC1512000); State Key Laboratory of Geo-Information Engineering (Grant No. SKLGIE2022-ZZ2-07); The Fundamental Research Funds for the Central Universities (CHD300102263715). This research has also been partially funded by the project "GENESIS: GNSS Environmental and Societal Missions – Subproject UPC", Grant PID2021-126436OB-C21 funded by the Ministerio de Ciencia e Investigación (MCIN)/Agencia Estatal de Investigación (AEI)/10.13039/501100011033 and EU FEDER "Una manera de hacer Europa". Zhongmin Ma's work was partly supported by the China Scholarship Council (CSC) through a State Scholarship Fund (No. 202306560073).

6. REFERENCES

[1] X. Li et al., "Analysis of coastal wind speed retrieval from CYGNSS mission using artificial neural network," *Remote Sens. Environ.*, vol. 260, Jul. 2021, doi: 10.1016/j.rse.2021.112454.

[2] C. Wang et al., "Significant Wave Height Retrieval Based on Multivariable Regression Models Developed with CYGNSS Data,"

IEEE Trans. Geosci. Remote Sens., vol. 61, pp. 1-15, 2023, Art no. 4200415, doi: 10.1109/TGRS.2022.3233102.

[3] A. Camps et al., "Sensitivity of GNSS-R spaceborne observations to soil moisture and vegetation," *IEEE J. Sel. Topics Appl. Earth Observ. Remote Sens.*, vol. 9, no. 10, pp. 4730-4742, Oct. 2016, doi: 10.1109/JSTARS.2016.2588467.

[4] H. Carreno-Luengo, G. Luzi and M. Crosetto, "Above-ground biomass retrieval over tropical forests: A novel GNSS-R approach with CyGNSS", *Remote Sens.*, vol. 12, no. 9, pp. 1368, Apr. 2020, doi: 10.3390/rs12091368.

[5] C. Chew, J. T. Reager and E. Small, "CYGNSS data map flood inundation during the 2017 Atlantic hurricane season", *Sci. Rep.*, vol. 8, pp. 9336, Jun. 2018, doi: 10.1038/s41598-018-27673-x.

[6] S. Zhang et al., "Using CYGNSS data to map flood inundation during the 2021 extreme precipitation in Henan province China," *Remote Sens.*, vol. 13, no. 24, pp. 5181, Dec. 2021, doi: 10.3390/rs13245181.

[7] W. Li, E. Cardellach, F. Fabra, S. Ribo and A. Rius, "Lake level and surface topography measured with spaceborne GNSS-Reflectometry from CYGNSS mission: Example for the Lake Qinghai", *Geophys. Res. Lett.*, vol. 45, pp. 13 332–13 341, 2018, doi: 10.1029/2018GL080976.

[8] J. Zhang and Y. J. Morton, "Inland Water Body Surface Height Retrievals Using CYGNSS Delay Doppler Maps," *IEEE Trans. Geosci. Remote Sens.*, vol. 61, pp. 1-16, 2023, Art no. 4209316, doi: 10.1109/TGRS.2023.3330410.

[9] A. Betterle, and S. Peter. "A parsimonious approach to estimate flood depths—also in urban areas—for satellite-based flood maps," *No. EGU23-1603. Copernicus Meetings*, 2023, doi: 10.5194/egusphere-egu23-1603.

[10] Jeffrey Neal, Laurence Hawker (2023): FABDEM V1-2. https://doi.org/10.5523/bris.s5hqmjcdj8yo2ibzi9b4ew3sn

[11] CYGNSS. 2021. CYGNSS Level 1 Science Data Record Version 3.1. Ver. 3.1. PO. DAAC, CA, USA. Dataset accessed [2023-12-01] at https://doi.org/10.5067/CYGNS-L1X31

[12] A. Camps and J. F. Munoz-Martin, "Analytical computation of the spatial resolution in GNSS-R and experimental validation at L1 and L5", *Remote Sens.*, vol. 12, no. 23, pp. 3910, 2020, doi: https://doi.org/10.3390/rs12233910.

[13] H. Carreno-Luengo and A. Camps, "Unified GNSS-R formulation including coherent and incoherent scattering components," *2016 IEEE International Geoscience and Remote Sensing Symposium (IGARSS)*, Beijing, China, 2016, pp. 4815-4818, doi: 10.1109/IGARSS.2016.7730256.

[14] A. Alonso-Arroyo, V. U. Zavorotny and A. Camps, "Sea ice detection using U.K. TDS-1 GNSS-R data", *IEEE Trans. Geosci. Remote Sens.*, vol. 55, no. 9, pp. 4989-5001, Sep. 2017, doi: 10.1109/TGRS.2017.2699122.

[15] C. Gerlein-Safdi and C. S. Ruf, "A CYGNSS-based algorithm for the detection of inland waterbodies", *Geophysical Res. Lett*, vol. 46, pp. 12065-12072, 2019, doi: 10.1029/2019GL085134.

[16] M. M. Al-Khaldi et al., "Inland water body mapping using CYGNSS coherence detection", *IEEE Trans. Geosci. Remote Sens.*, vol. 59, no. 9, pp. 7385-7394, Sep. 2021, doi: 10.1109/TGRS.2020.3047075.

[17] Z. Ma et al., "CYGNSS High Spatiotemporal Resolution Flood Monitoring Based on POBI Interpolation: A Case Study of 2022 Pakistan Catastrophic Floods." *China Satellite Navigation Conference*. Singapore: Springer Nature Singapore, 2023, doi: 10.1007/978-981-99-6928-9_7.

[18] A. Camps, "Spatial resolution in GNSS-R under coherent scattering", *IEEE Geosci. Remote Sens. Lett.*, vol. 17, no. 1, pp. 32-36, Jan. 2019, doi: 10.1109/LGRS.2019.2916164.

[19] C. C. Chew, "Spatial interpolation based on previously-observed behavior: A framework for interpolating spaceborne GNSS-R data from CYGNSS," *J. Spatial Sci.*, pp. 1-14, Jun. 2021, doi: 10.1080/14498596.2021.1942253.

[20] S. Zhang et al., " POBI interpolation algorithm for CYGNSS near real time flood detection research: A case study of extreme precipitation events in Henan, China in 2021," *Adv. Space Res.*, vol. 71, no. 6, pp. 2862-2878, Feb. 2023, doi: 10.1016/j.asr.2022.11.016.

[21] A. L. Neuenschwander, K. L. Pitts, B. P. Jelley, J. Robbins, J. Markel, S. C. Popescu, R. F. Nelson, D. Harding, D. Pederson, B. Klotz, and R. Sheridan. (2023). ATLAS/ICESat-2 L3A Land and Vegetation Height, Version 6 [Data Set]. Boulder, Colorado USA. NASA National Snow and Ice Data Center Distributed Active Archive Center. https://doi.org/10.5067/ATLAS/ATL08.006. Date Accessed 01-01-2024.

[22] H. Park et al., "Retracking considerations in spaceborne GNSS-R altimetry", *GPS Solut.*, vol. 16, no. 4, pp. 507-518, Jan. 2012. doi: 10.1007/s10291-011-0251-7.